NASA TECHNICAL NOTE

NASA TN D-7265

NASA TN D-7265

GAS-PHASE HYDROGEN PERMEATION THROUGH ALPHA IRON, 4130 STEEL, AND 304 STAINLESS STEEL FROM LESS THAN 100° C TO NEAR 600° C

by Howard G. Nelson and James E. Stein

Ames Research Center
Moffett Field, Calif. 94035

NATIONAL AERONAUTICS AND SPACE ADMINISTRATION • WASHINGTON, D. C. • APRIL 1973

1. Report No.	2. Government Accession No.	3. Recipient's Catalog No.
NASA TN D-7265		

4. Title and Subtitle	5. Report Date
GAS-PHASE HYDROGEN PERMEATION THROUGH ALPHA IRON, 4130 STEEL, AND 304 STAINLESS STEEL FROM LESS THAN 100° C TO NEAR 600° C	April 1973
	6. Performing Organization Code
7. Author(s)	8. Performing Organization Report No.
Howard G. Nelson and James E. Stein	A-4749
	10. Work Unit No. 501-21-21-01-00-21
9. Performing Organization Name and Address	11. Contract or Grant No.
Ames Research Center Moffett Field, Calif. 94035	
	13. Type of Report and Period Covered
12. Sponsoring Agency Name and Address	Technical Note
National Aeronautics and Space Administration Washington, D. C. 20546	14. Sponsoring Agency Code

15. Supplementary Notes

16. Abstract

Gas-phase hydrogen permeation studies were conducted on hollow, cylindrical membranes of triply zone-refined alpha iron, AISI 304 austenitic stainless steel, and AISI-SAE 4130 steel in both the normalized (ferrite and carbide) and quenched and tempered (martensite) conditions. Membrane temperature was varied from less than 100° C to near 600° C and hydrogen pressure was varied from 1×10^{4} Nm^{-2} to 3×10^{6} Nm^{-2}. For one membrane material, normalized 4130 steel, gas-phase hydrogen transport under both steady-state and nonsteady-state conditions was demonstrated to be controlled by lattice diffusion. Additionally, Sievert's law was shown to be applicable. For all membrane materials, expressions for the coefficients for hydrogen permeation, ϕ, were determined by analysis of steady-state transport; the coefficients for diffusion, D, were determined by the lag-time technique applied to nonsteady-state transport; and through a knowledge of the Sievert's constants, the subsurface equilibrium lattice hydrogen concentrations, C, were determined.

17. Key Words (Suggested by Author(s))	18. Distribution Statement
Gaseous hydrogen Permeation Diffusion Solubility	Unclassified – Unlimited.

19. Security Classif. (of this report)	20. Security Classif. (of this page)	21. No. of Pages	22. Price*
Unclassified	Unclassified	21	$3.00

* For sale by the National Technical Information Service, Springfield, Virginia 22151

SYMBOLS

C	subsurface equilibrium hydrogen concentration (cm^3 (NTP)cm^{-3})
C_i	subsurface hydrogen concentration at the inside surface of a hollow, cylindrical membrane
C_o	subsurface hydrogen concentration at the outside surface of a hollow, cylindrical membrane
D	coefficient for hydrogen diffusion within the metal lattice (cm^2 s^{-1})
D_o	pre-exponential constant for hydrogen diffusion
j_t	overall hydrogen flow rate through a hollow, cylindrical membrane
K	Sievert's constant of proportionality
ℓ	length of a hollow, cylindrical membrane
P_i	hydrogen pressure on the inside of a hollow, cylindrical membrane
P_o	hydrogen pressure on the outside of a hollow, cylindrical membrane
Q_d	activation energy for hydrogen diffusion
Q_p	activation energy for hydrogen permeation
r_i	inside radius of a hollow, cylindrical membrane
r_o	outside radius of a hollow, cylindrical membrane
R	gas constant (J $kmole^{-1}$ $°K^{-1}$)
t_L	lag-time parameter for nonsteady-state transport (s)
T	absolute temperature of a hollow, cylindrical membrane
ϕ	coefficient for hydrogen permeation under steady-state conditions through the metal lattice (cm^3 (NTP) cm^{-1} s^{-1} $(Nm^{-2})^{-1/2}$)
ϕ_o	pre-exponential constant for hydrogen permeation

GAS-PHASE HYDROGEN PERMEATION THROUGH ALPHA IRON, 4130 STEEL, AND 304 STAINLESS STEEL FROM LESS THAN 100° C TO NEAR 600° C

Howard G. Nelson and James E. Stein

Ames Research Center

SUMMARY

Gas-phase hydrogen permeation studies were conducted on hollow, cylindrical membranes of triply zone-refined alpha iron, AISI 304 austenitic stainless steel, and AISI-SAE 4130 steel in both the normalized (ferrite and carbide) and quenched and tempered (martensite) conditions. Membrane temperature was varied from less than 100° C to near 600° C and hydrogen pressure was varied from 1×10^{4} Nm^{-2} to 3×10^{6} Nm^{-2}. For one membrane material, normalized 4130 steel, gas-phase hydrogen transport under both steady-state and nonsteady-state conditions was demonstrated to be controlled by lattice diffusion. Additionally, Sievert's law was shown to be applicable. For all membrane materials, expressions for the coefficients for hydrogen permeation, ϕ, were determined by analysis of steady-state transport; the coefficients for diffusion, D, were determined by the lag-time technique applied to nonsteady-state transport; and through a knowledge of the Sievert's constants, the subsurface equilibrium lattice hydrogen concentration, C, were determined.

INTRODUCTION

Several reviews are available on hydrogen transport in iron-base alloys (refs. 1-3). Aside from the phenomenological interest in the kinetic parameters involved in the transport process, an accurate knowledge of the rate of hydrogen transport in and through iron-base alloys is of considerable practical importance. For example, the rate processes of hydrogen transport are inherently involved in the phenomenon of hydrogen embrittlement of metals (ref. 4) – embrittlement either from hydrogen originally present in the metal lattice (ref. 5) or from an external environment, such as a high-purity hydrogen gas (ref. 6) or hydrogen-containing molecules (ref. 7). In fact, the rate processes of hydrogen transport can control whether or not an alloy will exhibit hydrogen embrittlement (ref. 8).

Although numerous studies have been conducted to determine the reaction kinetics of hydrogen transport through iron-base alloys, most have been limited to either high temperatures or to chemical or electrolytic techniques because of the sensitivity of the permeation apparatus. Additionally, many of the older data are unreliable because of the lack of system, material, and surface characterization. It is the purpose of this study to establish the kinetic rate equations for gas-phase hydrogen permeation, lattice diffusion, and equilibrium lattice solubility in a number of iron base alloys to as low a temperature as possible, using a highly sensitive gas-phase permeation apparatus. Membrane materials studied are triply zone-refined alpha iron, AISI 304 stainless steel, and AISI-SAE 4130 steel in the normalized and quenched and tempered conditions.

THEORETICAL CONSIDERATIONS

The kinetic parameters of permeability, diffusivity, and equilibrium solubility can be determined experimentally by the proper analysis of the steady-state and nonsteady-state portions of the simple penetration-rate-versus-time curves.

Permeation

If it is assumed that the overall hydrogen transport process under steady-state conditions is controlled by diffusion through the bulk material, that is, if the transport process is not affected by reactions occurring on the membrane surface, the overall flow rate of hydrogen through the walls of a cylindrical membrane is given by the equation (ref. 9):

$$j_t = \phi \frac{2\pi\ell}{(ln\, r_O - ln\, r_i)} \left(p_i^{1/2} - p_O^{1/2}\right) \tag{1}$$

Empirically, the flow rate, j_t, is also dependent on temperature. This temperature dependence enters equation (1) through the coefficient of permeation, ϕ, and is given in the form of the Arrhenius equation:

$$\phi = \phi_O \exp(-Q_p/RT) \tag{2}$$

Therefore, under steady-state conditions, where the hydrogen flow rate is constant with respect to time, the coefficient of hydrogen permeation can be determined through equation (1) and the variation of the steady-state flow rate with temperature will yield the kinetic parameters of equation (2).

Diffusion

Barrer (ref. 10) has developed a technique to measure the coefficient of diffusion by utilizing a nonsteady-state parameter known as lag-time, t_L. The lag-time determination is based on the rate of hydrogen concentration change in a constant volume at the exit side of a permeated membrane. The slope on a pressure-versus-time curve, corresponding to a constant rate of pressure rise (steady-state conditions), is extrapolated back to the initial pressure of the collection volume yielding a value of time. The increment in time from time zero (the instant in time the entrance surface of the membrane is exposed to hydrogen) is known as the lag-time.

The lag-time parameter has been expressed by Barrer (ref. 10) in terms of the coefficient of diffusion, D, for a cylindrical geometry as:

$$t_L = \frac{r_i^2 - r_O^2 + (r_i^2 + r_O^2)\, ln(r_O/r_i)}{4\, ln(r_O/r_i)} \frac{1}{D} \tag{3}$$

assuming that phase boundary reactions can be neglected, and that the boundary conditions to Fick's second law solution are constants corresponding to instantaneous equilibrium between the gas-phase hydrogen and hydrogen within the metal surface. The relationship between D and t_L is dependent solely on specimen geometry and thus, for a given membrane configuration:

$$D = \text{constant} \frac{1}{t_L} \tag{4}$$

Similar to the coefficient for permeation, the coefficient for diffusion is temperature dependent and is given in the form of the Arrhenius equation:

$$D = D_O \exp(-Q_d/RT) \tag{5}$$

Therefore, the determination of the kinetic parameters of diffusion is simply a matter of establishing the magnitude and temperature dependence of the lag-time parameter obtained from the penetration-rate-versus-time curves.

Solubility

Equilibrium hydrogen solubility is the subsurface hydrogen concentration in equilibrium with gas-phase hydrogen above that surface. Equilibrium hydrogen solubility, C, is empirically given by Sievert's law (ref. 11) which relates the atomic concentration just below the surface of a solid to the pressure of the diatomic gas above that surface:

$$C = Kp^{1/2} \tag{6}$$

Under steady-state conditions, the hydrogen concentrations at both the entrance and exit surfaces of the membrane will be constant with time and thus, the overall gas flow rate for a cylindrical membrane can be expressed by the following relationship obtained by integration of Fick's first law:

$$j_t = \frac{-D2\pi\ell}{(\ln r_O - \ln r_i)} (C_O - C_i) \tag{7}$$

Substituting equation (6) into equation (7), assuming $C_O \ll C_i$, and equating this result to equation (1), we obtain the expression for C_i, the equilibrium solubility just below the inner membrane surface, in terms of the experimentally determined coefficients of permeation and diffusion:

$$C_i = \frac{\phi}{D} p_i^{1/2} \tag{8}$$

APPARATUS AND MATERIAL

The experimental system used in these studies is similar to that developed by Frauenfelder (ref. 12). The test system as shown in figure 1 consists of two ultrahigh vacuum systems, an input system used for the introduction of hydrogen into the specimen, and an output system for the analysis and removal of the permeated hydrogen. All vacuum seals were metallic, with the exception of the viton "O"-ring compression type seal between the vacuum jacket and the specimen. This seal, cooled with liquid nitrogen cooling coils, permitted translational movement of the test piece in order to eliminate strains which would have otherwise developed as the result of thermal expansion of the specimen during heating and cooling.

The materials used in these studies were triply zone-refined alpha-iron, commercial AISI-SAE 4130 steel (nominal composition: 0.30 percent *C*, 0.70 percent *Cr*, and 0.20 percent *Mo*) having a normalized structure of ferrite and carbide and a quenched and tempered structure of martensite, and commercial AISI 304 austenitic stainless steel (nominal composition: 0.08 percent max *C*, 18 percent *Cr*, and 8 percent *Ni*). Test specimens were machined to the desired gage section dimensions (fig. 1), polished on 600 grit paper, and rinsed in alcohol before mounting in the test apparatus.

The rate of steady-state hydrogen flow through the cylindrical membrane was obtained by valving out the ion-pump on the input system and back-filling the system (including the internal specimen cavity) to the desired pressure with hydrogen which had been passed through a palladium diffuser. The mass spectrometer (quadrupole residual gas analyzer) in the output system was used to continuously monitor the hydrogen penetrating the membrane. The mass spectrometer was calibrated to give hydrogen flow rate by the standard "known-conductance" technique (ref. 13) and was capable of measuring a hydrogen flow rate less than 10^{13} molecules per second.

Nonsteady-state lag-time measurements were made in the following manner: Hydrogen was first introduced into a precalibrated reservoir. An isolation valve between the reservoir and the input system was opened, causing rapid pressurization of the specimen to a predetermined pressure. Simultaneously with specimen pressurization, the mass spectrometer began recording the hydrogen pressure in the output system. Initially the ion-pump in the output system was valved out to provide a fixed collection volume for lag-time measurements; however, it was determined experimentally later that because of the relatively slow pumping speed of this pump, the same information could be determined with the pump on; i.e., the removal of hydrogen at low pressures was negligible compared to the initial hydrogen flow rate penetrating the membrane. The lag-time results are presented without distinction as to whether the ion-pump was valved out or not.

To obtain the maximum steady-state hydrogen flow rate and reproducible results from membrane to membrane, it was found necessary to expose first the inside surface of a new membrane to hydrogen at a temperature between 500° C to 600° C for approximately one-half hour. This procedure is similar to that used by Gibson et al. (ref. 14) to activate stainless steel membranes. It appears that this treatment reduces the surface oxide which remains or is formed on the membrane surface following the polishing operation. If the inside surface of the membrane became contaminated for some reason during a test, it was found that surface clean-up resulting in original rates of hydrogen flow could be obtained by re-subjecting the membrane to this treatment.

RESULTS

In order to demonstrate that steady-state gas-phase hydrogen transport is controlled by lattice diffusion and is not affected by surface reactions in iron base alloys, hydrogen flow rate, j_t, was studied as a function of $1/\log (r_O/r_i)$, the configurational parameter of equation (1), for normalized 4130 steel membranes. Figure 2 shows the observed data determined at a constant hydrogen pressure and at three different temperatures. The lines drawn through these data were determined for the three temperatures by substituting into equation (1) the value of the coefficient of permeation determined (below) for this material in the present study, equation (12). Reasonable agreement is seen to exist between the experimental data and these solid curves.

Likewise, nonsteady-state hydrogen transport is not seen to be affected by reactions occurring on the normalized 4130 steel membrane surfaces. Figure 3 is a plot of the reciprocal of lag-time versus the configurational function of equation (3) for normalized 4130 steel membranes at a constant temperature. It can be seen from this figure that the reciprocal of the lag-time parameter is inversely proportional to the configurational parameter (i.e., variation in membrane thickness), as would be expected from equation (3). The line drawn through these data was obtained by the substitution of the coefficient of diffusion determined for this material in the present study, equation (13), and has a slope of −1.0.

The applicability of Sievert's law, equation (6), was also verified for all membrane materials of this study. In all cases, under steady-state conditions hydrogen flow rate was found to be approximately proportional to the square root of the hydrogen driving pressure over the pressure range investigated (from 1×10^4 Nm^{-2} to 3×10^6 Nm^{-2}), as would be expected from equation (1).

Alpha Iron

The coefficient of hydrogen permeation (eq. 2) determined from equation (1) for alpha iron is shown in figure 4. It is seen from this figure that the data obey a linear relation on this type plot and are therefore indicative of a single thermally activated process over the entire temperature range of this study. From the best-fit curve as determined by least-mean-squares analysis of all data, the coefficient of hydrogen permeation was found to obey the relation:

$$\phi = 8.04\times10^{-6} \exp(-34{,}300/RT) \tag{9}$$

A similar plot of the reciprocal of lag-time versus the reciprocal of temperature for an alpha-iron membrane is shown in figure 5. As seen from this figure, the data seem best represented by two line segments indicating a transition to a higher "apparent" activation energy for diffusion at lower temperatures. [This effect has been observed previously by others (refs. 15 and 16), has been observed in the 4130 steel membranes of the present study, and has been discussed in detail and shown to be an artifact of the test technique (refs. 17-19).] From the best-fit curve through all the data at the higher temperatures, above the "apparent" transition temperature, the coefficient of diffusion was found to obey the relation:

$$D = 2.33\times10^{-3} \exp(-6680/RT) \tag{10}$$

Based on the observed equations (9) and (10) and the relationship given by equation (8), the equilibrium lattice hydrogen concentration, at a given hydrogen pressure, can be expressed by the following relation:

$$C = 3.45\text{X}10^{-3}\ p^{1/2}\ \exp(-27{,}600/RT) \tag{11}$$

Normalized 4130 Steel

The coefficient of permeation observed for AISI-SAE steel in the normalized condition is shown in figure 6. From the best-fit curve of all data, the coefficient of hydrogen permeation is given by the relation:

$$\phi = 6.53\text{X}10^{-6}\ \exp(-39{,}700/RT) \tag{12}$$

The reciprocal of lag-time observed for AISI-SAE 4130 steel in the normalized condition is shown in figure 7. As was seen in a similar plot for alpha iron, a break occurs in figure 7 at the lower temperatures. From the best-fit curve through all data at the higher temperatures, the coefficient of diffusion is given by the relation:

$$D = 3.53\text{X}10^{-3}\ \exp(-12{,}600/RT) \tag{13}$$

Based on equation (12) and (13), the equilibrium lattice hydrogen concentration at a given hydrogen pressure is given by the relation:

$$C = 1.85\text{X}10^{-3}\ p^{1/2}\ \exp(-27{,}100/RT) \tag{14}$$

Quenched and Tempered 4130 Steel

The coefficient of permeation observed for quenced and tempered 4130 steel is shown in figure 8. From the best-fit curve of all data, the coefficient of hydrogen permeation is given by the relation:

$$\phi = 8.17\text{X}10^{-6}\ \exp(-35{,}200/RT) \tag{15}$$

The reciprocal of lag-time observed for quenched and tempered 4130 steel is shown in figure 9. Again, a break occurs in this figure at the lower temperatures. From the best-fit curve through all data at higher temperatures, the coefficient of diffusion is given by the relation:

$$D = 3.56\text{X}10^{-3}\ \exp(-7950/RT) \tag{16}$$

Based on equations (15) and (16), the equilibrium lattice hydrogen concentration at some hydrogen pressure is given by the relation:

$$C = 2.29\text{X}10^{-3}\ p^{1/2}\ \exp(-27{,}200/RT) \tag{17}$$

304 Stainless Steel

The coefficient of permeation observed for 304 austenitic stainless steel is shown in figure 10. From the best-fit curve of all data, the coefficient of hydrogen permeation is given by the relation:

$$\phi = 2.34\times10^{-4} \exp(-64{,}000/RT) \tag{18}$$

The reciprocal of lag-time observed for 304 austenitic stainless steel is shown in figure 11. From the best-fit curve through all data, the coefficient of diffusion is given by the relation:

$$D = 2.72\times10^{-2} \exp(-54{,}400/RT) \tag{19}$$

Based on equations (18) and (19), the equilibrium lattice hydrogen concentration at some hydrogen pressure is given by the relation:

$$C = 8.60\times10^{-3}\, p^{1/2} \exp(-9600/RT) \tag{20}$$

DISCUSSION

The overall process of hydrogen transport through a membrane involves a number of reaction processes, any one of which could control the rate of the overall process. It is imperative that the rate controlling reaction process be identified, if analytical relationships are to be meaningfully applied to the experimental data. It has been demonstrated previously for electrolytic and chemical methods (ref. 20) that both steady-state and nonsteady-state hydrogen transport through iron base alloys are controlled under most conditions by lattice diffusion; however, no such characterization has heretofore been established for gas-phase transport (refs. 21-23). In the present study, the agreement between the configurational dependence observed under steady-state (fig. 2) and nonsteady-state (fig. 3) conditions with those expected from equations (1) and (3), respectively, strongly suggest that here too, lattice diffusion is the rate controlling process.

Although numerous studies have been conducted on hydrogen transport through iron base alloys, most have been limited to either high temperatures or to chemical or electrolytic methods. Additionally, many of the older data are unreliable because of the lack of system, material, and surface characterization. In the present study, the use of a sensitive gas-phase permeation apparatus and improved system characterization has allowed the extension of data to lower temperatures, has improved the reliability of the kinetic expressions for hydrogen transport in alpha iron and 304 stainless steel, and has estabilished the relevant expressions for normalized and quenched and tempered 4130 steel. In order to establish the accuracy and reliability of the kinetic expressions determined in the present study, the observed expression for the coefficient of permeation in alpha iron (eq. (9)) can be compared with the best available expression from the literature. Gonzalez (ref. 24) has considered carefully most previously existing determinations of steady-state permeability of hydrogen in alpha iron for systematic errors, purity of iron, and general technique. The following equation is his choice of the best data available and represents a confidence level of 90 percent:

$$\phi = (9.1 \pm 1)\times10^{-6} \exp(-35{,}300 \pm 1700/RT) \tag{21}$$

and is in excellent agreement with that observed in the present study, that is,

$$\phi = 8.04\times10^{-6} \exp(-34{,}300/RT)$$

In the present study, the reciprocal of lag-time (diffusivity) was observed to decrease more rapidly with decreasing temperature at low temperatures than at high temperatures for alpha iron (fig. 5), for normalized 4130 steel (fig. 7), and for quenched and tempered 4130 steel (fig. 9). This behavior has previously been observed in carbon steel and in alpha iron (refs. 16 and 17). Considering the relationship between permeability and diffusivity, equation (8), and the lack of an observed break in the temperature dependences of permeation in these metals (figs. 4, 6, and 8), it can readily be seen that this low temperature behavior is a consequence of nonsteady-state transport. This conclusion has been suggested by others and has been discussed in detail by Oriani (ref. 19), who has developed an explanation involving local equilibrium during nonsteady-state transport between the diffusing hydrogen in ordinary lattice sites and that in extraordinary lattice sites, such as internal voids.

CONCLUSIONS

(1) Over the temperature and pressure ranges of this study, both steady-state and nonsteady-state gas-phase hydrogen transport through normalized 4130 steel membranes have been demonstrated to be controlled by lattice diffusion.

(2) Sievert's law was obeyed for all membranes tested.

(3) The reciprocal of lag-time (diffusivity) was observed to decrease more rapidly with decreasing temperature at lower temperatures for alpha iron, normalized 4130 steel, and quenched and tempered 4130 steel membranes. As proposed previously, this anomalous behavior appears to be a consequence of nonsteady-state test conditions.

(4) Expressions were determined for the coefficient of hydrogen permeation by analysis of steady-state transport, for the coefficients of diffusion by the lag-time technique applied to nonsteady-state transport, and for subsurface equilibrium lattice hydrogen concentrations through Sievert's law:

for alpha iron

$$\phi = 8.04\times10^{-6} \exp(-34{,}300/RT)$$

$$D = 2.33\times10^{-3} \exp(-6680/RT)$$

$$C = 3.45\times10^{-3}\, p^{1/2} \exp(-27{,}600/RT)$$

for normalized 4130 steel

$$\phi = 6.53\times10^{-6} \exp(-39{,}700/RT)$$

$$D = 3.53\times10^{-3} \exp(-12{,}600/RT)$$

$$C = 1.85\times10^{-3}\, p^{1/2} \exp(-27{,}100/RT)$$

for quenched and tempered 4130 steel

$$\phi = 8.17 \times 10^{-6} \exp(-35{,}200/RT)$$

$$D = 3.56 \times 10^{-3} \exp(-7{,}950/RT)$$

$$C = 2.29 \times 10^{-3} \, p^{1/2} \exp(-27{,}200/RT)$$

and for 304 stainless steel

$$\phi = 2.34 \times 10^{-4} \exp(-64{,}000/RT)$$

$$D = 2.72 \times 10^{-2} \exp(-54{,}400/RT)$$

$$C = 8.6 \times 10^{-3} \, p^{1/2} \exp(-9{,}600/RT)$$

Ames Research Center
National Aeronautics and Space Administration
Moffett Field, Calif., January 10, 1973

REFERENCES

1. Oriani, R. A.: Hydrogen in Metals. Fundamental Aspects of Stress Corrosion Cracking. Natl. Assoc. of Corrosion Engrs., Houston, Texas, 1969, pp. 32-49.

2. Krishtal, M. A.: Diffusion Processes in Iron Alloys. Israel Prog. Sci. Translations, Israel, 1970 (available from OTS, U.S. Dept. Com. TT 770-50031).

3. Fast, Johan D.: Interaction of Metals and Gases. Academic Press, 1965.

4. Nelson, Howard G.: The Kinetic and Mechanical Aspects of Hydrogen-Induced Failure in Metals. NASA TN D–6691, 1972.

5. Tetelman, Alan S.: The Mechanism of Hydrogen Embrittlement in Steel. Fundamental Aspects of Stress Corrosion Cracking. Natl. Assoc. of Corrosion Engrs., Houston Texas, 1969, pp. 446-460.

6. Nelson, Howard G.; Williams, Dell P.; and Tetelman, Alan S.: Embrittlement of a Ferrous Alloy in a Partially Dissociated Hydrogen Environment. Met. Trans., vol. 2, April 1971, pp. 953-959.

7. Johnson, H. H.; and Willner, A. M.: Moisture and Stable Crack Growth in a High Strength Steel. Appl. Mat. Res., vol. 4, Jan. 1965, pp. 34-40.

8. Nelson, H. G.: Testing for Hydrogen Embrittlement: Primary and Secondary Influences. ASTM, Special Technical Publication, to be published in 1973.

9. Crank, John: The Mathematics of Diffusion. Oxford Press (London), 1964.

10. Barrer, Richard M.: Diffusion In and Through Solids. Cambridge Press (Cambridge), 1941.

11. Sieverts, A.: Absorption of Gases by Metals. Z. Metalkunde, vol. 21, 1929, pp. 37-46.

12. Frauenfelder, R.: Permeation of Hydrogen Through Tungsten and Molybdenum. J. Chem. Physics, vol. 48, 1968, pp. 3955-3965.

13. Dushman, Saul: Scientific Foundations of Vacuum Technique. Wiley and Sons, 1958, p. 80.

14. Gibson, R.; Jones, P. M. S.; and Evans, J. A.: The Permeation and Diffusion of Hydrogen Isotopes through Stainless Steel. Great Britain Atomic Weapons Research Establishment Report No. AWRE-0-47/65, 1965.

15. Barrer, R. M.: Stationary and Non-Stationary States of Flow of Hydrogen in Palladium and Iron. Trans. Faraday Soc. vol. 36, 1940, pp. 1235-1248.

16. Johnson, E. W.; and Hill, M. L.: The Diffusivity of Hydrogen in Alpha Iron. Trans. AIME, vol. 218, 1960, pp. 1104-1112.

17. Ono, Kanji; and Rosales, L. A.: The Anomalous Behavior of Hydrogen in Iron at Lower Temperatures. Trans. Met. Soc., AIME, vol. 242, 1968, pp. 244-248.

18. Chew, B.: A Void Model for Hydrogen Diffusion in Steel. J. Metal Sci. vol. 5, 1971, pp. 195-200.

19. Oriani, Richard A.: Diffusion and Trapping of Hydrogen in Steel. Acta Met., vol. 18, 1970, pp. 147-157.

20. Beck, W.; Bockris, J. O'M., McBreen, J.; and Nanis, L.: Hydrogen Permeation in Metals as a Function of Stress, Temperature and Dissolved Hydrogen Concentration. Royal Soc. (London), Series A., vol. 290, 1966, pp. 220-235.

21. Frank, Robert C.; Swets, Don E.; and Fry, David L.: Mass Spectrometer Measurements of the Diffusion Coefficient of Hydrogen in Steel in the Temperature Range of 25° – 90° C. J. Appl. Physics, vol. 29, 1958, pp. 892-898.

22. Eschbach, H. L.; Gross, F.; and Schulien, S.: Permeability for Various Steels. Vacuum, vol. 13, 1963, pp. 543-547.

23. Gonzalez, O. D.: Permeation of Hydrogen and Deuterium in Alpha Iron. Trans. AIME, vol. 239, 1967, pp. 929-930.

24. Gonzalez, O. D.: The Measurement of Hydrogen Permeation in Alpha Iron: An Analysis of the Experiments. Trans. Met. Soc. AIME, vol. 245, 1969, pp. 607-612.

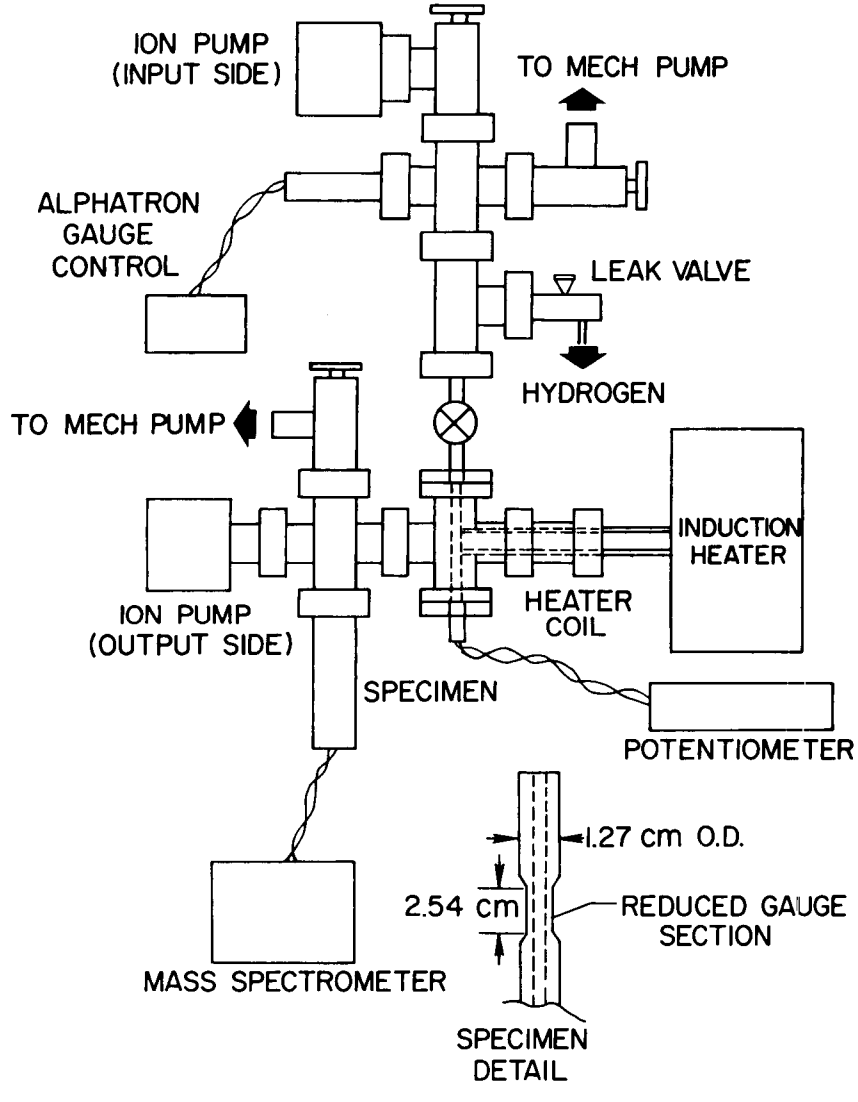

Figure 1.– Permeation system assembly and components.

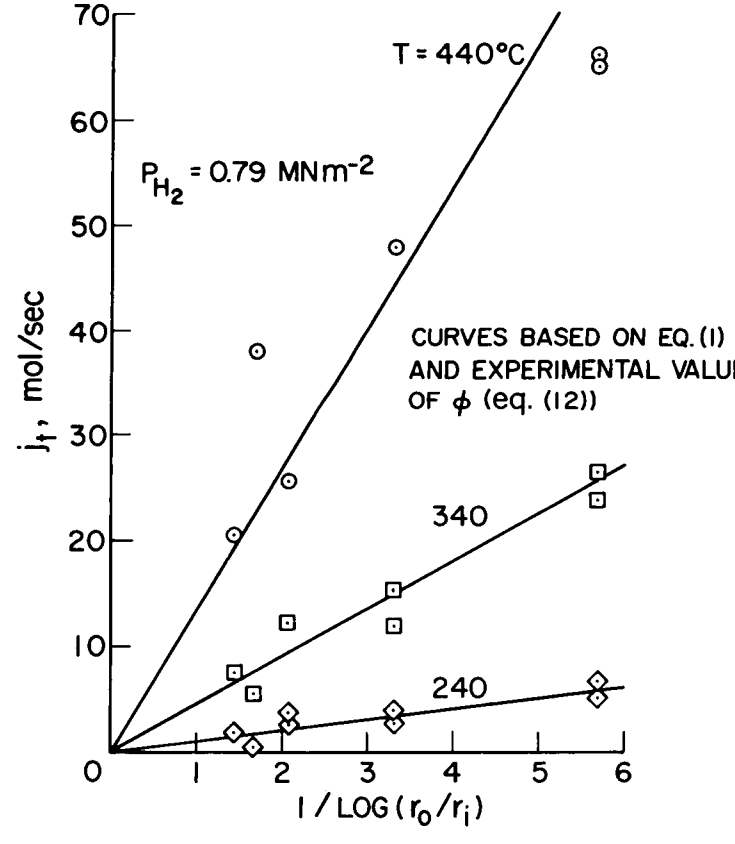

Figure 2.– Hydrogen flow rate through normalized 4130 steel as a function of inner and outer radius.

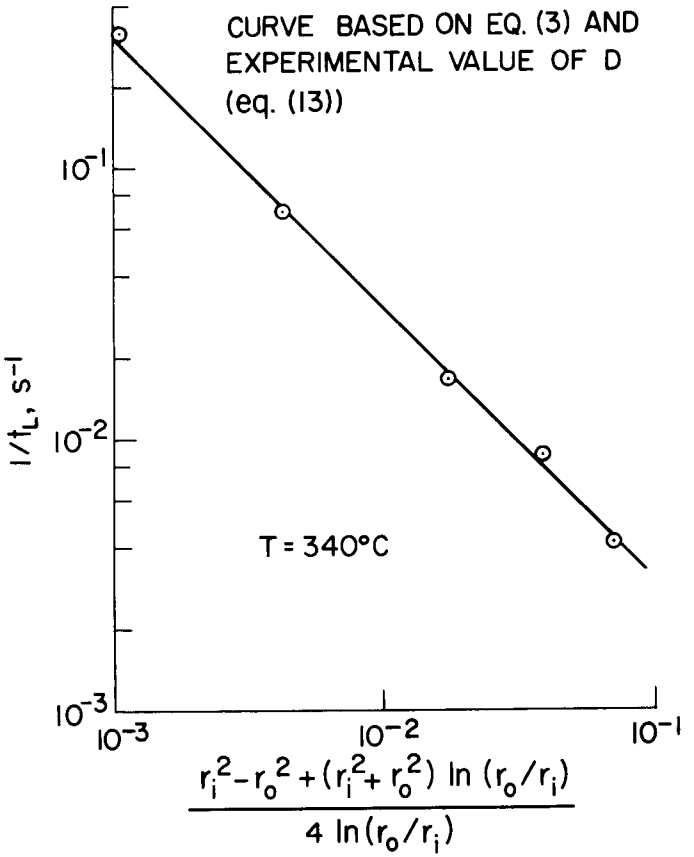

Figure 3.– Lag-time parameter as a function of inner and outer radii in normalized 4130 steel.

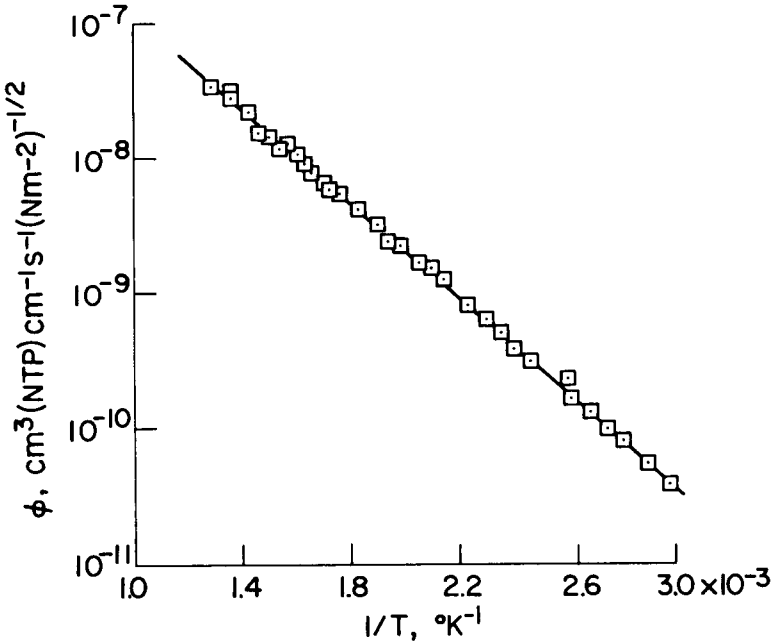

Figure 4.– The effect of temperature on the coefficient of hydrogen permeation in alpha iron.

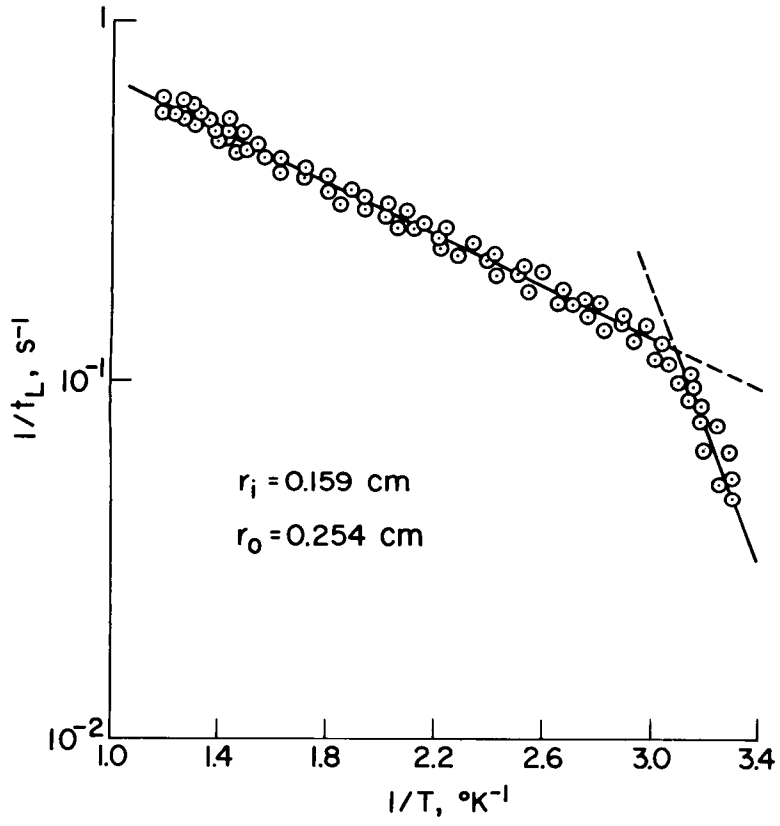

Figure 5.– The effect of temperature on the reciprocal of lag-time in alpha iron.

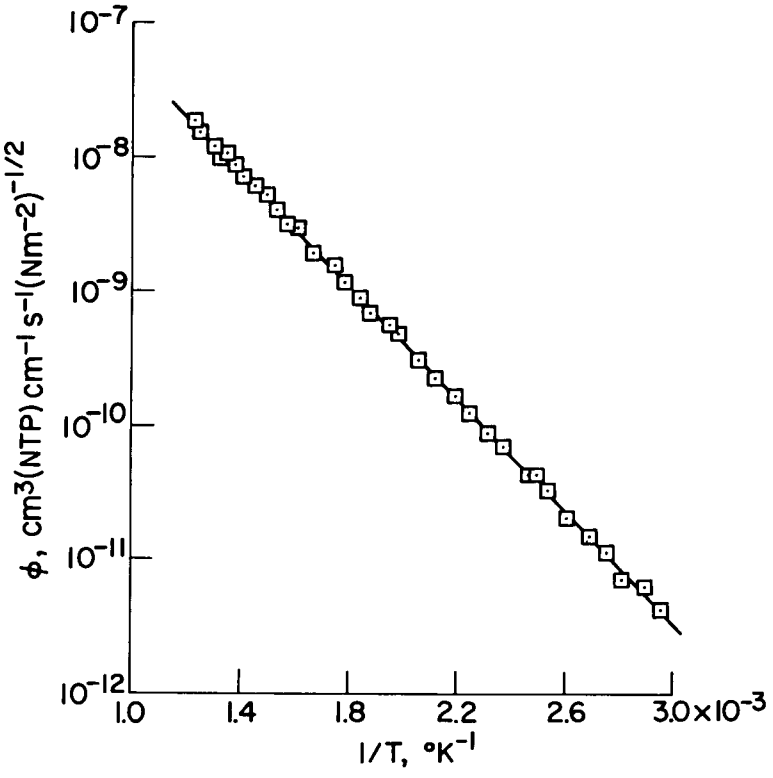

Figure 6.– The effect of temperature on the coefficient of hydrogen permeation in normalized 4130 steel.

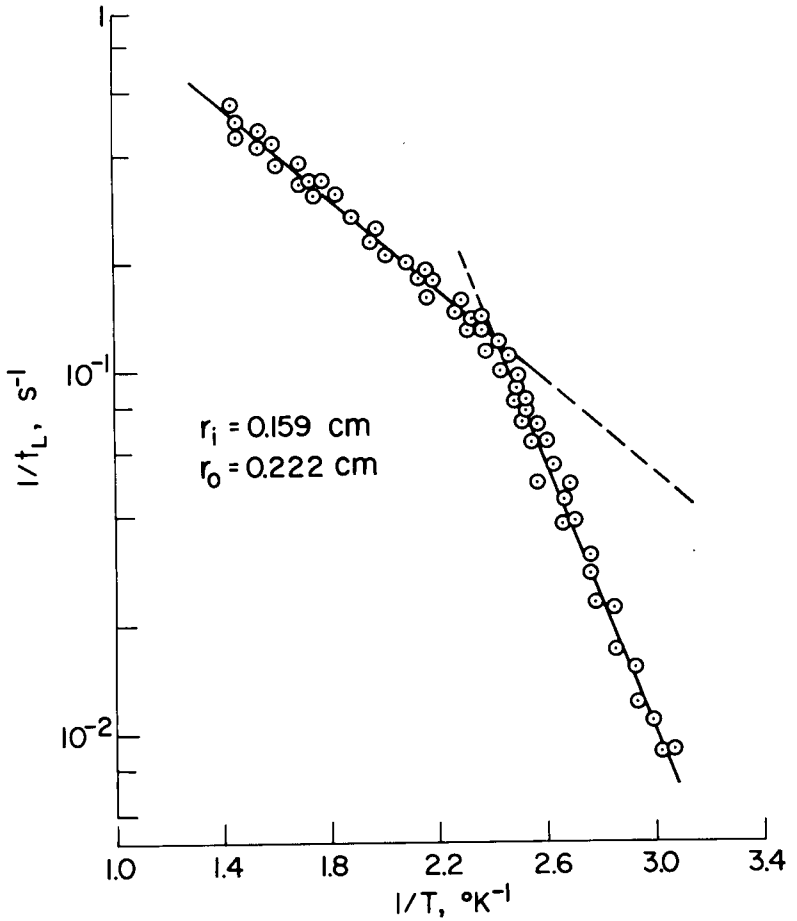

Figure 7.– The effect of temperature on the reciprocal of lag-time in normalized 4130 steel.

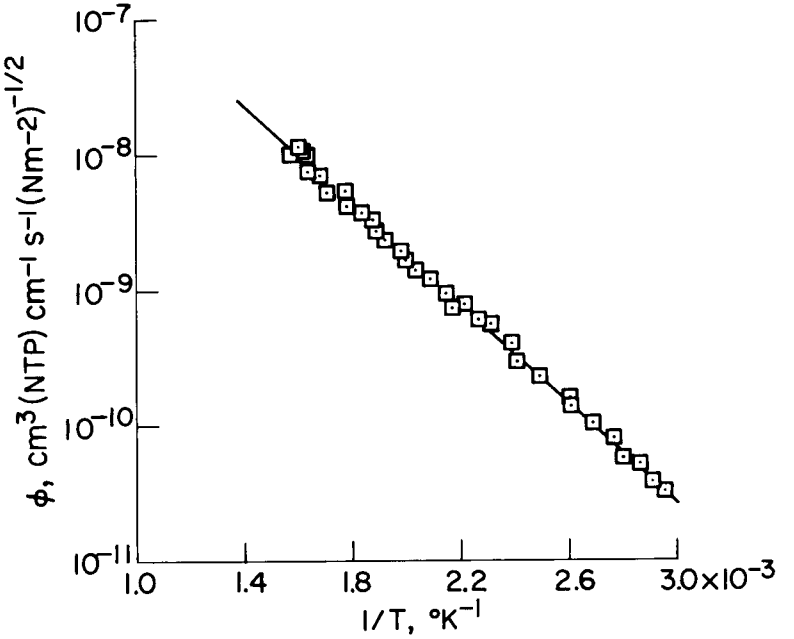

Figure 8.– The effect of temperature on the coefficient of hydrogen permeation in quenched and tempered 4130 steel.

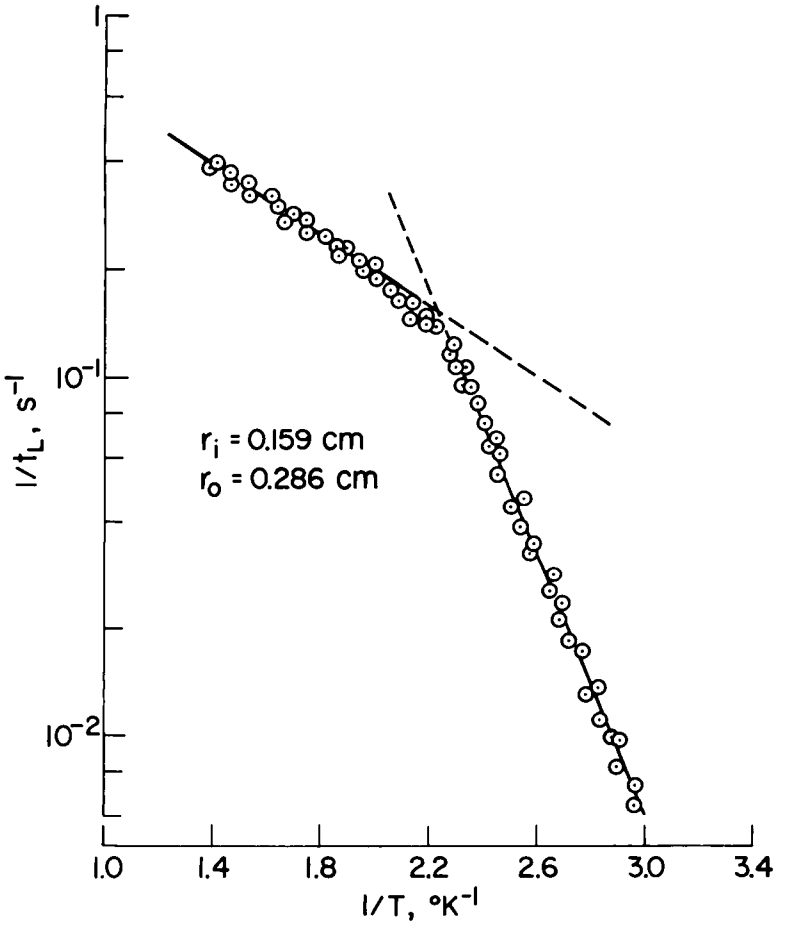

Figure 9.– The effect of temperature on the reciprocal of lag-time in quenched and tempered 4130 steel.

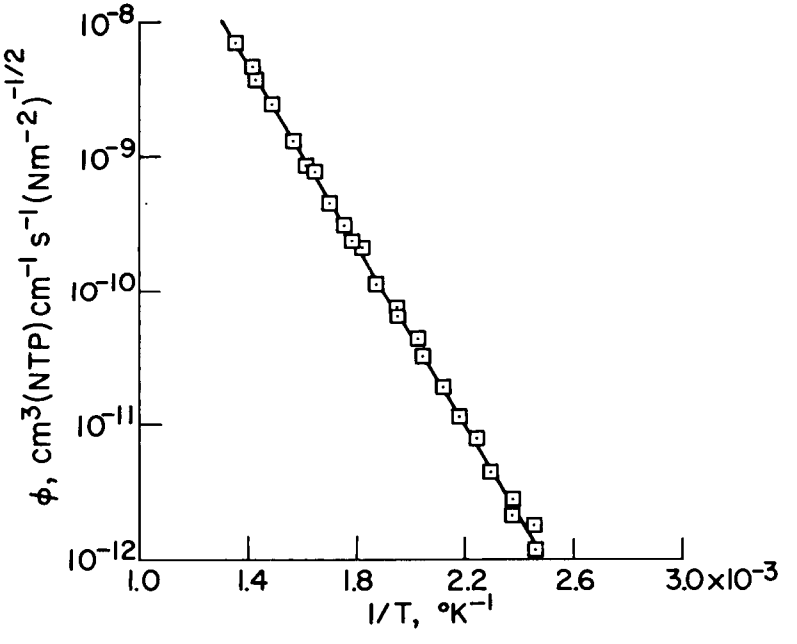

Figure 10.– The effect of temperature on the coefficient of hydrogen permeation in 304 stainless steel.

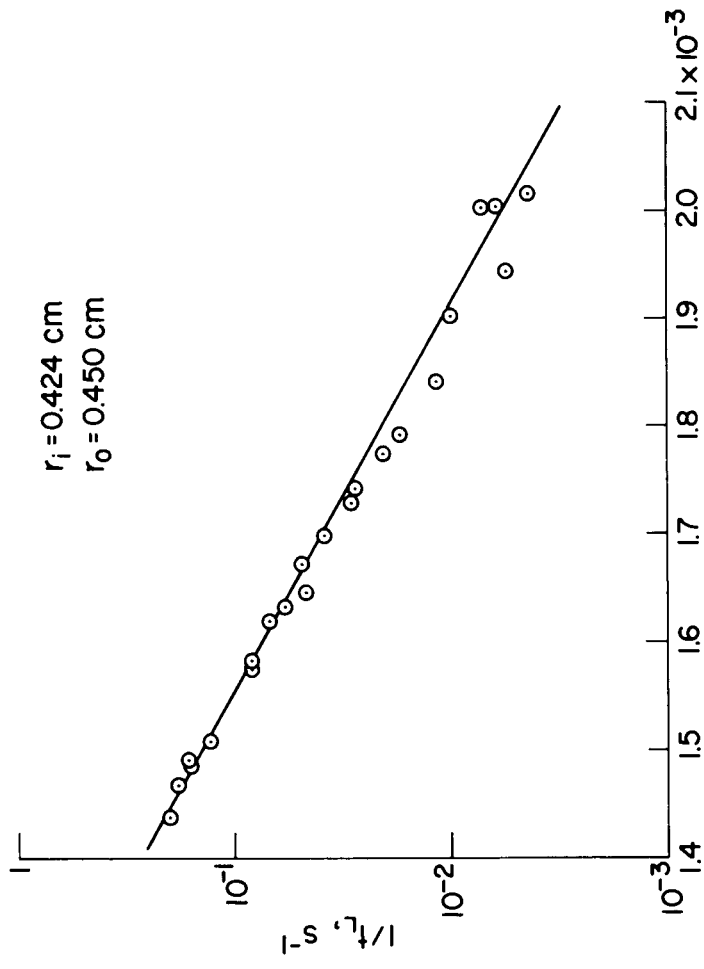

Figure 11.— The effect of temperature on the reciprocal of lag-time in 304 stainless steel.

NASA-Langley, 1973 — 17 A-4749